Transverse shear deformation in multicell box beam bridges

Autor(en): **Robertson, J.C. / Pama, R.P. / Cusens, A.R.**

Objekttyp: **Article**

Zeitschrift: **IABSE publications = Mémoires AIPC = IVBH Abhandlungen**

Band (Jahr): **30 (1970)**

PDF erstellt am: **21.07.2024**

Persistenter Link: https://doi.org/10.5169/seals-23597

Nutzungsbedingungen

Die ETH-Bibliothek ist Anbieterin der digitalisierten Zeitschriften. Sie besitzt keine Urheberrechte an den Inhalten der Zeitschriften. Die Rechte liegen in der Regel bei den Herausgebern.
Die auf der Plattform e-periodica veröffentlichten Dokumente stehen für nicht-kommerzielle Zwecke in Lehre und Forschung sowie für die private Nutzung frei zur Verfügung. Einzelne Dateien oder Ausdrucke aus diesem Angebot können zusammen mit diesen Nutzungsbedingungen und den korrekten Herkunftsbezeichnungen weitergegeben werden.
Das Veröffentlichen von Bildern in Print- und Online-Publikationen ist nur mit vorheriger Genehmigung der Rechteinhaber erlaubt. Die systematische Speicherung von Teilen des elektronischen Angebots auf anderen Servern bedarf ebenfalls des schriftlichen Einverständnisses der Rechteinhaber.

Haftungsausschluss

Alle Angaben erfolgen ohne Gewähr für Vollständigkeit oder Richtigkeit. Es wird keine Haftung übernommen für Schäden durch die Verwendung von Informationen aus diesem Online-Angebot oder durch das Fehlen von Informationen. Dies gilt auch für Inhalte Dritter, die über dieses Angebot zugänglich sind.

Ein Dienst der *ETH-Bibliothek*
ETH Zürich, Rämistrasse 101, 8092 Zürich, Schweiz, www.library.ethz.ch

http://www.e-periodica.ch

Transverse Shear Deformation in Multicell Box Beam Bridges

Déformations latérales dues au cisaillement des poutres en caisson multicellulaire

Schubverformung in Querrichtung von mehrzelligen Kastenträger-Brücken

J. C. ROBERTSON
BSc, Research Assistant, University of Dundee

R. P. PAMA
PhD, Research Fellow, University of Dundee

A. R. CUSENS
PhD, Professor of Civil Engineering, University of Dundee

Notation

a	spacing of webs in box-beam section
b	half-width of bridge
c	position of load from the support
D_1	coupling rigidity per unit length of the bridge
D_2	coupling rigidity per unit width of the bridge
D_x	flexural rigidity per unit width of the bridge
D_y	flexural rigidity per unit length of the bridge
D_{xy}	torsional rigidity per unit width of the bridge
D_{yx}	torsional rigidity per unit length of the bridge
E	elastic modulus
G	shear modulus
h	overall depth of bridge
I	second moment of area
J	torsional second moment
$2H$	total torsional rigidity of the bridge
H_n	load function
L	span of bridge
M_x	longitudinal bending moment per unit width of the bridge
M_y	transverse bending moment per unit length of the bridge
M_{xy}	torsional moment per unit width of the bridge
M_{yx}	torsional moment per unit length of the bridge

n harmonic
R_x longitudinal reactive force per unit width of the bridge
R_y transverse reactive force per unit length of the bridge
S_B shear stiffness
V_x longitudinal shear per unit width of the bridge
V_y transverse shear per unit length of the bridge
w total vertical deflection
w_B deflection due to bending
w_S deflection due to shear
y_p distance of station from the load
α torsional parameter
α_s effective torsional parameter
α_n parameter dependent on the harmonic
η_1 dimensionless parameter defining the left hand edge of the bridge
η_2 dimensionless parameter defining the right hand edge of the bridge
θ flexural parameter
θ_S effective flexural parameter
γ shearing strain

Introduction

The box section beam is finding increasing application in bridge construction. The section is relatively light in weight but strong in torsion and flexure. A bridge deck which is composed of a multi-cell box section (six or more cells)

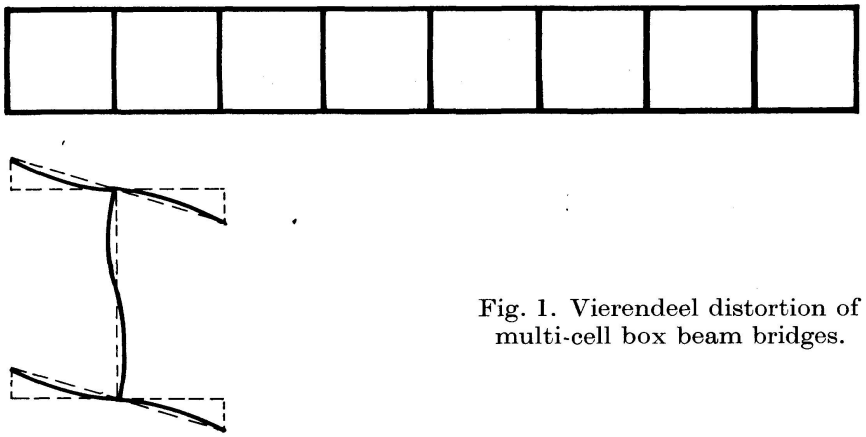

Fig. 1. Vierendeel distortion of multi-cell box beam bridges.

may be analysed as an orthotropic plate by conventional methods [1, 2, 3]. However if the webs or flanges of the box are slender, distortion of the cross-section is likely to occur in the absence of transverse diaphragms. Fig. 1 illustrates the deformation of the transverse cross-section in the manner of a vierendeel frame. Such vierendeel distortion will cause an increase in both deflection and longitudinal moment values in the proximity of concentrated

loads. MASSONNET and GANDOLFI [4] have drawn attention to this effect and showed that increases in deformation can be dramatic in the case of shear-weak sections. They also suggest a semi-empirical approach to the determination of deflection and moment in practical cases. More recently, SAWKO and COPE [5] have also considered shear distortion in box beams using a limited approach based on the assumption of a plane stress condition in the flanges of the box.

In a large proportion of practical designs of multi-cell box beam bridge decks significant shear distortion of the transverse cross-section will not occur but clearly neglect of this effect in all cases could have serious implications. In this paper the Huber orthotropic plate equation is modified by the introduction of an additional parameter to account for shear distortion. The resulting differential equations are solved by the use of half-range Fourier series and a general method of analysis is developed for the determination of deflections, moments and shears in a simply supported multi-cell box-section bridge deck under concentrated or line loads.

Theoretical Analysis

In addition to the customary assumptions made in the analysis of elastic plates, the following assumptions are made:

1. The total deflection of the deck is equal to the sum of the deflections due to bending and shear, i.e.

$$w = w_B + w_S, \tag{1}$$

where w is the total deflection; w_B and w_S are the deflections due to bending and shear respectively.

2. The transverse shear is equal to the product of the shear stiffness and the slope of the shear deformation in the transverse direction

$$V_y = S_B\left(\frac{\partial w_S}{\partial y}\right), \tag{2}$$

where S_B is the shear stiffness of the deck. The value of S_B is explained later in the section on elastic rigidities of the deck.

3. The curvature of the deck in the longitudinal direction is derived from the total deflection while for the transverse direction it is derived from the deflection due to bending only.

Thus,

$$\phi_x = \frac{\partial^2 w}{\partial x^2}, \tag{3}$$

$$\phi_y = \frac{\partial^2 w_B}{\partial y^2}. \tag{4}$$

It follows from this assumption that the longitudinal and transverse bending moments are

$$M_x = -\left[D_x \frac{\partial^2 w}{\partial x^2} + D_1 \frac{\partial^2 w_B}{\partial y^2}\right], \tag{5}$$

$$M_y = -\left[D_y \frac{\partial^2 w_B}{\partial y^2} + D_2 \frac{\partial^2 w}{\partial x^2}\right]. \tag{6}$$

The twisting moments in the two orthogonal directions x and y are obtained from the shearing strain

$$\gamma = \frac{\partial^2 w}{\partial x\, \partial y} - \frac{1}{S_B}\left(\frac{\partial V_y}{\partial x}\right). \tag{7}$$

From Eq. (2) this may be expressed as

$$\gamma = \left(\frac{\partial^2 w}{\partial x\, \partial y} - \frac{\partial^2 w_S}{\partial x\, \partial y}\right) = \frac{\partial^2 w_B}{\partial x\, \partial y}. \tag{8}$$

Hence the shearing strain is a function of the deformation due to bending only and the twisting moments become

$$M_{xy} = D_{xy}\gamma = D_{xy} \frac{\partial^2 w_B}{\partial x\, \partial y}, \tag{9}$$

$$M_{yx} = -D_{yx}\gamma = -D_{yx} \frac{\partial^2 w_B}{\partial x\, \partial y}. \tag{10}$$

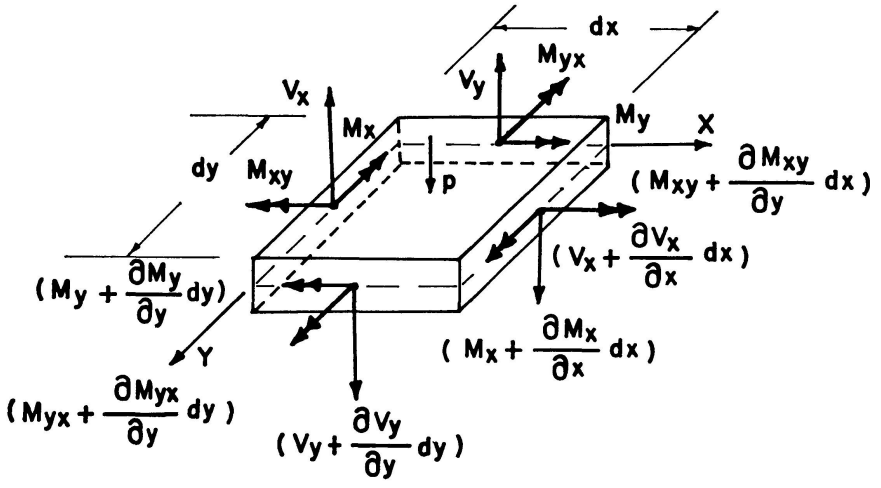

Fig. 2. Free-body diagram of an element of the deck.

From these moment-curvature relationships, the shearing and reactive forces (see Fig. 2) may be shown to be

$$V_x = \left(\frac{\partial M_x}{\partial x} + \frac{\partial M_{yx}}{\partial y}\right) = -\left[D_x \frac{\partial^3 w}{\partial x^3} + (D_{yx} + D_1) \frac{\partial^3 w_B}{\partial x\, \partial y^2}\right], \tag{11}$$

$$V_y = \left(\frac{\partial M_y}{\partial y} + \frac{\partial M_{xy}}{\partial x}\right) = -\left[D_y \frac{\partial^3 w_B}{\partial y^3} + D_2 \frac{\partial^3 w}{\partial x^2\, \partial y} + D_{xy} \frac{\partial^3 w_B}{\partial x^2\, \partial y}\right], \tag{12}$$

$$R_x = \left(V_x - \frac{\partial M_{xy}}{\partial y}\right) = -\left[D_x \frac{\partial^3 w}{\partial x^3} + (D_{xy} + D_{yx} + D_1) \frac{\partial^3 w_B}{\partial x \partial y^2}\right], \tag{13}$$

$$R_y = \left(V_y + \frac{\partial M_{yx}}{\partial x}\right) = -\left[D_y \frac{\partial^3 w_B}{\partial y^3} + D_2 \frac{\partial^3 w}{\partial x^2 \partial y} + (D_{xy} + D_{yx}) \frac{\partial^3 w_B}{\partial x^2 \partial y}\right]. \tag{14}$$

Consideration of the equilibrium of the vertical forces and the summation of moments in the two orthogonal directions leads to the usual equation for elastic plates

$$\frac{\partial^2 M_x}{\partial x^2} + \frac{\partial^2 M_y}{\partial y^2} + \frac{\partial^2 M_{yx}}{\partial x \partial y} - \frac{\partial^2 M_{xy}}{\partial x \partial y} = -p(x, y). \tag{15}$$

In terms of the deflections w and w_B this equation may be expressed as

$$D_x \frac{\partial^4 w}{\partial x^4} + (D_1 + D_{xy} + D_{yx}) \frac{\partial^4 w_B}{\partial x^2 \partial y^2} + D_2 \frac{\partial^4 w}{\partial x^2 \partial y^2} + D_y \frac{\partial^4 w_B}{\partial y^4} = p(x, y). \tag{16}$$

It is apparent from this expression that if $w_B = w$, the equation reduces to the HUBER orthotropic plate equation [6].

The slopes in the transverse direction may be expressed as

$$\frac{\partial w}{\partial y} = \frac{\partial w_B}{\partial y} + \frac{\partial w_S}{\partial y}. \tag{17}$$

From Eqs. (2) and (12),

$$\frac{\partial w}{\partial y} = \frac{\partial w_B}{\partial y} + \frac{V_y}{S_B} \tag{18}$$

or

$$\frac{\partial w}{\partial y} = \frac{\partial w_B}{\partial y} - \frac{1}{S_B}\left[D_y \frac{\partial^3 w_B}{\partial y^3} + D_2 \frac{\partial^3 w}{\partial x^2 \partial y} + D_{xy} \frac{\partial^3 w_B}{\partial x^2 \partial y}\right]. \tag{19}$$

The equation may be re-arranged into the form

$$S_B \frac{\partial w}{\partial y} - S_B \frac{\partial w_B}{\partial y} + D_y \frac{\partial^3 w_B}{\partial y^3} + D_2 \frac{\partial^3 w}{\partial x^2 \partial y} + D_{xy} \frac{\partial^3 w_B}{\partial x^2 \partial y} = 0. \tag{20}$$

Thus, the three original basic assumptions result in two simultaneous differential Eqs. (16) and (20) in w and w_B. If the load and deflections are expressed in half-range Fourier sine series, for the nth harmonic of the series the contributions to the total and bending deflections may be written as

$$w_n = W_n \sin \alpha_n x, \tag{21}$$

$$w_{Bn} = W_{Bn} \sin \alpha_n x, \tag{22}$$

where

$$\alpha_n = \frac{n\pi}{L}. \tag{23}$$

and L is the span of the deck.

The complete solution may be split into homogeneous and particular parts. For the homogeneous part, the following ordinary differential equations are

obtained if Eqs. (21) and (22) are substituted into Eqs. (16) and (20), with $p(x, y)$ set to zero:

$$\alpha_n^4 D_x W_n - \alpha_n^2 D_2 \frac{d^2 W_n}{dy^2} - \alpha_n^2 (D_1 + D_{xy} + D_{yx}) \frac{d^2 W_{Bn}}{dy^2} + D_y \frac{d^4 W_{Bn}}{dy^4} = 0, \quad (24)$$

$$S_B \frac{dW_n}{dy} - S_B \frac{dW_{Bn}}{dy} + D_y \frac{d^3 W_{Bn}}{dy^3} - \alpha_n^2 D_2 \frac{dW_n}{dy} - \alpha_n^2 D_{xy} \frac{dW_{Bn}}{dy} = 0. \quad (25)$$

Using the operator notation

$$D^m = \frac{d^m}{dy^m}, \quad (26)$$

these two equations may be expressed in matrix form as follows

$$\left[\begin{array}{c|c} \alpha_n^4 D_x - \alpha_n^2 D_2 D^2 & -\alpha_n^2 (D_1 + D_{xy} + D_{yx}) D^2 + D_y D^4 \\ \hline S_B D - \alpha_n^2 D_2 D & -(S_B + \alpha_n^2 D_{xy}) D + D_y D^3 \end{array}\right] \left[\begin{array}{c} W_n \\ \hline W_{Bn} \end{array}\right] = \left[\begin{array}{c} 0 \\ \hline 0 \end{array}\right]. \quad (27)$$

For a non-trivial solution, the determinant of Eq. (27) must be zero, hence

$$\{(-S_B D_y D^5) + [\alpha_n^4 D_x D_y + \alpha_n^2 D_2 S_B + \alpha_n^4 D_2 D_{xy} + \alpha_n^2 S_B (D_1 + D_{xy} + D_{yx}) - \alpha_n^4 D_2 (D_1 + D_{xy} + D_{yx})] D^3 + [-\alpha_n^4 D_x S_B - \alpha_n^6 D_x D_y] D\} \begin{bmatrix} W_n \\ W_{Bn} \end{bmatrix} = \begin{bmatrix} 0 \\ 0 \end{bmatrix}. \quad (28)$$

For simplicity, the following substitutions are made:

$$2H^* = (D_1 + D_{xy} + D_{yx}), \quad (29)$$

$$P_1 = -S_B D_y, \quad (30)$$

$$P_2 = S_B (D_2 + 2H^*) + \alpha_n^2 [D_x D_y - D_2 (D_1 + D_{yx})], \quad (31)$$

$$P_3 = -D_x (S_B + \alpha_n^2 D_{xy}) \quad (32)$$

and the operator equation may be written as

$$\{(P_1 D^5 + \alpha_n^2 P_2 D^3 + \alpha_n^4 P_3 D)\} \begin{bmatrix} W_n \\ W_{Bn} \end{bmatrix} = \begin{bmatrix} 0 \\ 0 \end{bmatrix}. \quad (33)$$

The absence of the term in D^0 implies that the total deflection function is of the form

$$w = w_B + w_S + c \ (= \text{constant}).$$

For this to be compatible with Eq. (1), the constant c must be zero which implies that the power of the operator equation may be reduced by one, thus

$$\{P_1 D^4 + \alpha_n^2 P_2 D^2 + \alpha_n^4 P_3\} \begin{bmatrix} W_n \\ W_{Bn} \end{bmatrix} = \begin{bmatrix} 0 \\ 0 \end{bmatrix}. \quad (34)$$

Consider now an ordinary differential equation of the type

$$P_1 \frac{d^4 W_n}{dy^4} + \alpha_n^2 P_2 \frac{d^2 W_n}{dy^2} + \alpha_n^4 P_3 W_n = 0 \quad (35)$$

and assume a solution of the form

$$W_n = A\, e^{(\alpha_n s)y}, \tag{36}$$

where A is an arbitrary constant. Upon substitution into Eq. (35), the characteristic equation is obtained as

$$P_1(\alpha_n s)^4 + \alpha_n^2 P_2(\alpha_n s)^2 + \alpha_n^4 P_3 = 0. \tag{37}$$

The roots may be evaluated by quadratic formula and the expression for the quantity s of the roots may be obtained as

$$s = \pm\sqrt{\left(\frac{-P_2}{2P_1}\right) \pm \sqrt{\left(\frac{-P_2}{2P_1}\right)^2 - \left(\frac{P_3}{P_1}\right)}}. \tag{38}$$

The four roots are $+(\alpha_n s_1)$, $+(\alpha_n s_2)$, $-(\alpha_n s_1)$ and $-(\alpha_n s_2)$. This may be generally represented as $\pm\alpha_n s_j$ so that j will have values of 1 and 2 only.

Introducing a parameter α_s such that

$$\alpha_s = \frac{(D_{xy} + D_{yx} + D_1 + D_2) + \frac{\alpha_n^2}{S_B}[D_x D_y - D_2(D_1 + D_{yx})]}{2\sqrt{D_x D_y\left(1 + \frac{\alpha_n^2 D_{xy}}{S_B}\right)}}, \tag{39}$$

the quantity s_j of the root may be simplified as

$$s_j = \sqrt[4]{\frac{D_x}{D_y}\left(1 + \frac{\alpha_n^2 D_{xy}}{S_B}\right)}\sqrt{\alpha_s \pm \sqrt{\alpha_s^2 - 1}}. \tag{40}$$

Upon inspection of Eq. (40) it becomes apparent that another parameter is identified as

$$\theta_s = \frac{b}{L}\sqrt[4]{\frac{D_x}{D_y}\left(1 + \frac{\alpha_n^2 D_{xy}}{S_B}\right)}. \tag{41}$$

These parameters α_s and θ_s are the equivalents of the torsional and flexural parameter α and θ originally by MASSONNET [2] for use in the conventional orthotropic plate theory. It follows that

$$\lim_{S_B \to \infty} \alpha_s = \frac{(D_{xy} + D_{yx} + D_1 + D_2)}{2\sqrt{D_x D_y}} = \alpha \tag{42}$$

and

$$\lim_{S_B \to \infty} \theta_s = \frac{b}{L}\sqrt[4]{\frac{D_x}{D_y}} = \theta. \tag{43}$$

Clearly the parameters α_s and θ_s vary with the harmonic hence a generalized notation will be employed in the solution.

Solution of the Orthotropic Plate Equation

Consider a bridge deck of span L and width $2b$ as an orthotropic plate simply supported along the ends $x = 0$ and $x = L$. The complete solution of the

non-homogeneous Eq. (16) may be obtained by adding the homogeneous and particular parts of the solution,

$$w = w^h + w^p . \tag{44}$$

The letters h and p will be used as superscript or subscript as appropriate to denote the quantities associated with the homogeneous and particular parts respectively. w^p is the particular part of the solution obtained by considering the effect of the loading. This does not in general satisfy all the boundary conditions. w^h, the homogeneous part is added to give the complete solution. The homogeneous part has to satisfy the equation without the lateral load $p(x, y)$ but with the boundary forces acting on it.

Homogeneous Solution

The roots of the characteristic equation may be real or complex and exist in pairs denoted by $+(\alpha_n s_j)$ and $-(\alpha_n s_j)$ where j has values 1 and 2. The amplitude of the deflection function may be written as

$$w^h = \sum_{j=1}^{2} (A_j^h e^{-\alpha_n s_j y_h} + A_{j+2}^h e^{+\alpha_n s_j y_h}), \tag{45}$$

$$w_B^h = \sum_{j=1}^{2} (B_j^h e^{-\alpha_n s_j y_h} + B_{j+2}^h e^{+\alpha_n s_j y_h}). \tag{46}$$

For the homogeneous solution, the distance of the reference station measured transversely from the longitudinal centre line of the deck is denoted by y_h. Stations to the right of the centre line are considered positive and those to the left as negative.

The relationships between the arbitrary constants in Eq. (45) and (46) may be established from the conditional Eq. (25) if these deflection functions are substituted into it, thus

$$\begin{aligned}(S_B - \alpha_n^2 D_2)(-\alpha_n s_j A_j^h e^{-\alpha_n s_j y_h}) + (S_B - \alpha_n^2 D_2)(\alpha_n s_j A_{j+2}^h e^{+\alpha_n s_j y_h}) \\ -[S_B - D_y \alpha_n^2 s_j^2 + \alpha_n^2 D_{xy}](-\alpha_n s_j B_j^h e^{-\alpha_n s_j y_h}) \\ -[S_B - D_y \alpha_n^2 s_j^2 + \alpha_n^2 D_{xy}](\alpha_n s_j B_{j+2}^h e^{+\alpha_n s_j y_h}) = 0 .\end{aligned} \tag{47}$$

Collecting all terms which are functions of $e^{-\alpha_n s_j y_h}$ and equating them to zero, an equation is obtained relating the arbitrary constants A_j^h and B_j^h,

$$B_j^h = A_j^h \frac{(S_B - \alpha_n^2 D_2)}{(S_B - D_y \alpha_n^2 s_j + \alpha_n^2 D_{xy})}. \tag{48}$$

The same relationship may be shown to exist between B_{j+2}^h and A_{j+2}^h if all terms containing $e^{+\alpha_n s_j y_h}$ are collected and equated to zero.

Setting

$$F W_j = \frac{B_j^h}{A_j^h} = \frac{B_{j+2}^h}{A_{j+2}^h} = \frac{(S_B - \alpha_n^2 D_2)}{(S_B - D_y \alpha_n^2 s_j + \alpha_n^2 D_{xy})} \tag{49}$$

the deflection functions for the homogeneous part may be written as follows:

$$w^h = \sum_{n=1}^{\infty} \sin \alpha_n x \sum_{j=1}^{2} (A_j^h e^{-\alpha_n s_j y_h} + A_{j+2}^h e^{+\alpha_n s_j y_h}), \tag{50}$$

$$w_B^h = \sum_{n=1}^{\infty} \sin \alpha_n x \sum_{j=1}^{2} F W_j (A_j^h e^{-\alpha_n s_j y_h} + A_{j+2}^h e^{+\alpha_n s_j y_h}). \tag{51}$$

It may be shown from Eq. (49) that the

$$\lim_{S_B \to \infty} F W_j = \frac{B_j^h}{A_j^h} = \frac{B_{j+2}^h}{A_{j+2}^h} = 1 \tag{52}$$

and the bending deflection is equal to the total deflection of the deck.

Particular Solution

An infinitely wide bridge deck, as seen in Fig. 3 under the action of a line load expressed in sinusoidal form, will be used in evaluating the deflection

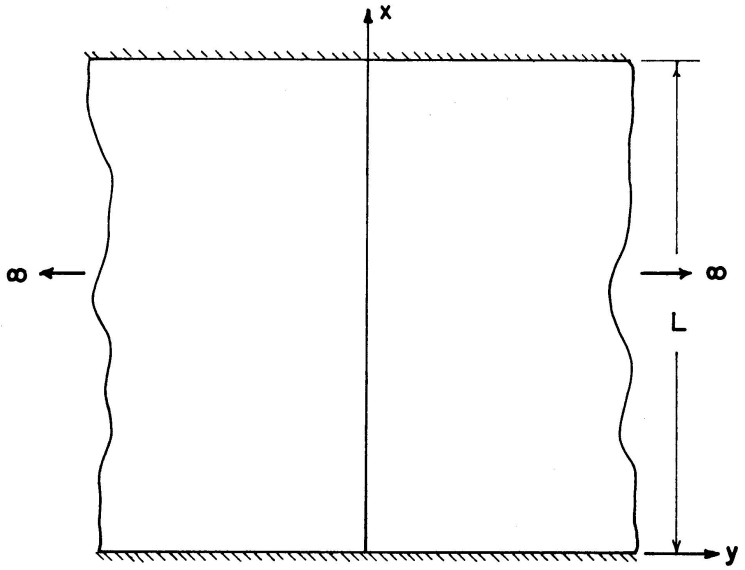

Fig. 3. Coordinate axis for infinitely wide bridge deck.

function w^p. For the particular part, the deflections may be expressed as

$$w^p = \sum_{n=1}^{\infty} \sin \alpha_n x \sum_{j=1}^{2} (A_j^p e^{-\alpha_n s_j y_p} + A_{j+2}^p e^{+\alpha_n s_j y_p}), \tag{53}$$

$$w_B^p = \sum_{n=1}^{\infty} \sin \alpha_n x \sum_{j=1}^{2} (B_j^p e^{-\alpha_n s_j y_p} + B_{j+2}^p e^{+\alpha_n s_j y_p}), \tag{54}$$

where the arbitrary constants are identified by the superscript p. The transverse distance of the station from the load is denoted by y_p. To preserve the symmetry of the system, an absolute value will be used for y_p thus an adjustment in sign is necessary for anti-symmetric quantities such as R_y for example. This will be fully explained later.

For the deflection function and its derivates to vanish at distances far from the load, the positive pairs of the roots $\alpha_n s_j$ will be discarded and the remaining expressions are simplified to the forms

$$w^p = \sum_{n=1}^{\infty} \sin \alpha_n x \sum_{j=1}^{2} A_j^p e^{-\alpha_n s_j y_p}, \tag{55}$$

$$w_B^p = \sum_{n=1}^{\infty} \sin \alpha_n x \sum_{j=1}^{2} B_j^p e^{-\alpha_n s_j y_p}. \tag{56}$$

Since the same conditional equation applies to the homogeneous and particular solutions, the arbitrary constants B_j^p and A_j^p are related in the same way as B_j^h and A_j^h, and hence the particular parts of the deflection functions may also be written in terms of the factor $F W_j$

$$w^p = \sum_{n=1}^{\infty} \sin \alpha_n x \sum_{j=1}^{2} A_j^p e^{-\alpha_p s_j y_p}, \tag{57}$$

$$w_B^p = \sum_{n=1}^{\infty} \sin \alpha_n x \sum_{j=1}^{2} F W_j A_j^p e^{-\alpha_n s_j y_p}. \tag{58}$$

The two arbitrary constants ($A_{j=1}^p$ and $A_{j=2}^p$) are obtained from the two boundary conditions under the load, namely:

1. For each harmonic, the slope of the bending deflection in the transverse direction is zero,

i. e.
$$\left(\frac{\partial w_B^p}{\partial y}\right)_{y_p=0} \tag{59}$$

and by substitution of Eq. (58)

$$\sum_{j=1}^{\infty} F W_j s_j A_j^p = 0. \tag{60}$$

2. The reactive force under the load is equal to half the load. If the applied load is expressed in half-range Fourier sine series, then for each harmonic

$$(R_y^p)_{y_p=0} = -\frac{H_n}{2} \sin \alpha_n x, \tag{61}$$

where H_n is a load function which may be derived for any form of load. This boundary condition may be expressed in terms of the deflection functions as follows:

$$-\left[D_y \frac{\partial^3 w^p}{\partial y^3} + (D_{xy} + D_{yx}) \frac{\partial^3 w^p}{\partial x^2 \partial y} + D_2 \frac{\partial^3 w^p}{\partial x^2 \partial y}\right] = -\frac{H_n}{2} \sin \alpha_n x \tag{62}$$

or
$$\sum_{j=1}^{2} A_j^p [D_y \alpha_n^3 s_j^3 F W_j - (D_{xy} + D_{yx}) \alpha_n^3 s_j F W_j - D_2 \alpha_n^3 s_j] = -\frac{H_n}{2}. \tag{63}$$

For simplicity, the term inside the bracket of Eq. (63) may be replaced by $F R_{yj}$, thus

$$F R_{yj} = [D_y \alpha_n^3 s_j^3 F W_j - (D_{xy} + D_{yx}) \alpha_n^3 s_j F W_j - D_2 \alpha_n^3 s_j] \tag{64}$$

and the two arbitrary constants are determined accordingly.

Complete Solution

The complete solutions for w and w_B are obtained by adding the homogeneous and particular solutions:

$$w = \sum_{n=1}^{\infty} \sin \alpha_n x \sum_{j=1}^{2} [A_j^p e^{-\alpha_n s_j y_p} + A_j^h e^{-\alpha_n s_j y_h} + A_{j+2}^h e^{+\alpha_n s_j y_h}], \tag{65}$$

$$w_B = \sum_{n=1}^{\infty} \sin \alpha_n x \sum_{j=1}^{2} F W_j [A_j^p e^{-\alpha_n s_j y_p} + A_j^h e^{-\alpha_n s_j y_h} + A_{j+2}^h e^{+\alpha_n s_j y_h}]. \tag{66}$$

Both deflection functions are symmetrical and it is therefore convenient to use the notation $S Y_j$ for the function inside the bracket of Eqs. (65) and (66), so that

$$S Y_j = (A_j^p e^{-\alpha_n s_j y_p} + A_j^h e^{-\alpha_n s_j y_h} + A_{j+2}^h e^{+\alpha_n s_j y_h}). \tag{67}$$

It must be emphasized here that the term $S Y_j$ is a function of the number of the harmonic, the value of j and also the transverse positions of both the load and the reference station. The deflection functions may be simply written as

$$w = \sum_{n=1}^{\infty} \sin \alpha_n x \sum_{j=1}^{2} S Y_j, \tag{68}$$

$$w_B = \sum_{n=1}^{\infty} \sin \alpha_n x \sum_{j=1}^{2} F W_j S Y_j. \tag{69}$$

The distance y_p of the station from the load is an absolute value as already mentioned in the derivation of the particular solution. This means that for a symmetrical function such as w, the contribution of the particular part $A_j^p e^{-\alpha_n s_j y_p}$ requires no change of sign. However, for antisymmetrical functions such as M_{xy}, M_{yx}, V_y and R_y, it is necessary to consider the particular part as

$$K A_j^p e^{-\alpha_n s_j y_p},$$

where K has the value of $+1$ if the station is to the right of the load and -1 if it is situated to the left.

Consider the anti-symmetric reactive force R_y such that

$$\begin{aligned} R_y = \sum_{n=1}^{\infty} \sin \alpha_n x \sum_{j=1}^{2} (&F R_{yj} K A_j^p e^{-\alpha_n s_j y_p} \\ &+ F R_{yj} A_j^h e^{-\alpha_n s_j y_h} + F R_{yj+2} A_{j+2}^h e^{+\alpha_n s_j y_h}). \end{aligned} \tag{70}$$

The quantity $F R_{yj+2}$ may be obtained from the expression for $F R_{yj}$ by replacing s_j by $-s_j$. It then becomes apparent that

$$F R_{yj+2} = -F R_{yj}. \tag{71}$$

This change of sign is consistent for all anti-symmetric functions mentioned earlier on since each is dependent on an odd power of the root $\alpha_n s_j$. Thus, the

term inside the bracket of Eq. (70) may be replaced by a simple notation $A\,S\,Y_j$ so that

$$A\,S\,Y_j = F\,R_{yj}\,(K\,A_j^p\,e^{-\alpha_n s_j y_p} + A_j^h\,e^{-\alpha_n s_j y_p} - A_{j+2}^h\,e^{+\alpha_n s_j y_p}). \tag{72}$$

With these notations $S\,Y_j$ and $A\,S\,Y_j$, the deflections, moments, twists, shears and reactive forces may be expressed in an abbreviated form.

Boundary Conditions

The four arbitrary constants of the homogeneous solution are obtained from the boundary conditions at the edges of the deck. If the deck is elastically

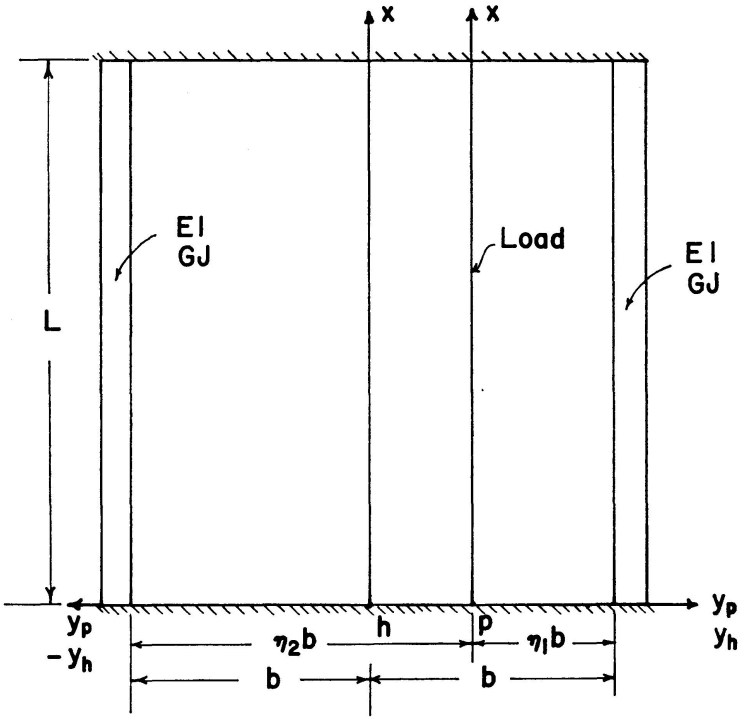

Fig. 4. Coordinate axes.

restrained by edge beams of flexural rigidity $E\,I$ and torsional rigidity $G\,J$ as shown in Fig. 4, the boundary conditions may be written as

$$(R_y^p)_{y_p=\eta_1 b} + (R_y^h)_{y_h=b} = -E\,I\left[\left(\frac{\partial^4 w^p}{\partial x^4}\right)_{y_p=\eta_1 b} + \left(\frac{\partial^4 w^h}{\partial x^4}\right)_{y_h=b}\right], \tag{73}$$

$$(R_y^p)_{y_p=\eta_2 b} + (R_y^h)_{y_h=-b} = +E\,I\left[\left(\frac{\partial^4 w^p}{\partial x^4}\right)_{y_p=\eta_2 b} + \left(\frac{\partial^4 w^h}{\partial x^4}\right)_{y_h=-b}\right], \tag{74}$$

$$(M_y^p)_{y_p=\eta_1 b} + (M_y^h)_{y_h=b} = +G\,J\left[\left(\frac{\partial^3 w^p}{\partial x^2\,\partial y}\right)_{y_p=\eta_1 b} + \left(\frac{\partial^3 w^h}{\partial x^2\,\partial y}\right)_{y_h=b}\right], \tag{75}$$

$$(M_y^p)_{y_p=\eta_2 b} + (M_y^h)_{y_h=-b} = -G\,J\left[\left(\frac{\partial^3 w^p}{\partial x^2\,\partial y}\right)_{y_p=\eta_2 b} + \left(\frac{\partial^3 w^h}{\partial x^2\,\partial y}\right)_{y_h=-b}\right], \tag{76}$$

$$\sum_{j=1}^{2}\{(F\,R_{yj}+\alpha_n^4\,E\,I)\;\;[A_j^p\,e^{-\eta_1\beta_j}+A_j^h\,e^{-\beta_j}]\;\;-(F\,R_{yj}-\alpha_n^4\,E\,I)\,A_{j+2}^h\,e^{\beta_j}\}\;\;=0\,,\quad(77)$$

$$\sum_{j=1}^{2}\{(F\,R_{yj}+\alpha_n^4\,E\,I)\;\;[A_j^p\,e^{-\eta_2\beta_j}+A_{j+2}^h\,e^{-\beta_j}]-(F\,R_{yj}-\alpha_n^4\,E\,I)\,A_j^h\,e^{\beta_j}\}\;\;=0\,,\quad(78)$$

$$\sum_{j=1}^{2}\{(F\,M_{yj}-\alpha_n^3\,s_j\,G\,J)[A_j^p\,e^{-\eta_1\beta_j}+A_j^h\,e^{-\beta_j}]\;\;+(F\,M_{yj}+\alpha_n^3\,s_j\,G\,J)\,A_{j+2}^h\,e^{\beta_j}\}=0\,,\quad(79)$$

$$\sum_{j=1}^{2}\{(F\,M_{yj}-\alpha_n^3\,s_j\,G\,J)[A_j^p\,e^{-\eta_2\beta_j}+A_{j+2}^h\,e^{-\beta_j}]+(F\,M_{yj}+\alpha_n^3\,s_j\,G\,J)\,A_j^h\,e^{\beta_j}\}\;\;=0\,,\quad(80)$$

where
$$\beta_j=\alpha_n\,s_j\,b \tag{81}$$

and
$$F\,M_{yj}=(D_2\,\alpha_n^2-D_y\,\alpha_n^2\,s_j^2\,F\,W_j)\,. \tag{82}$$

Thus the four arbitrary constants are determined by solving these four equations simultaneously. With the deflections w and w_B known, the bending and twisting moments, shearing and reactive forces are determined by successive differentiation. These are summarized as follows:

Deflection

Total:
$$w\;\;=\sum_{n=1}^{\infty}\sin\alpha_n\,x\sum_{j=1}^{2}S\,Y_j\,. \tag{83}$$

Bending:
$$w_B\;=\sum_{n=1}^{\infty}\sin\alpha_n\,x\sum_{j=1}^{2}F\,W_j\,(S\,Y_j)\,. \tag{84}$$

Longitudinal Bending Moment:
$$M_x\;=\sum_{n=1}^{\infty}\sin\alpha_n\,x\sum_{j=1}^{2}F\,M_{xj}\,S\,Y_j\,. \tag{85}$$

Transverse Bending Moment:
$$M_y\;=\sum_{n=1}^{\infty}\sin\alpha_n\,x\sum_{j=1}^{2}F\,M_{yj}\,S\,Y_j\,. \tag{86}$$

Transverse Twisting Moment:
$$M_{xy}=\sum_{n=1}^{\infty}\cos\alpha_n\,x\sum_{j=1}^{2}F\,M_{xyj}\,A\,S\,Y_j\,. \tag{87}$$

Longitudinal Twisting Moment:
$$M_{yx}=\sum_{n=1}^{\infty}\cos\alpha_n\,x\sum_{j=1}^{2}F\,M_{yxj}\,A\,S\,Y_j\,. \tag{88}$$

Longitudinal Shearing Force:
$$V_x\;\;=\sum_{n=1}^{\infty}\cos\alpha_n\,x\sum_{j=1}^{2}F\,V_{xy}\,S\,Y_j\,. \tag{89}$$

Transverse Shearing Force:
$$V_y\;\;=\sum_{n=1}^{\infty}\sin\alpha_n\,x\sum_{j=1}^{2}F\,V_{yj}\,A\,S\,Y_j\,. \tag{90}$$

Longitudinal Reactive Force:

$$R_x = \sum_{n=1}^{\infty} \cos \alpha_n x \sum_{j=1}^{2} F R_{xj} S Y_j . \tag{91}$$

Transverse Reactive Force:

$$R_y = \sum_{n=1}^{\infty} \sin \alpha_n x \sum_{j=1}^{2} F R_{yj} A S Y_j . \tag{92}$$

The quantities $F R_{yj}$ and $F M_{yj}$ have been defined earlier and the rest are given as follows:

$$F M_{xj} = (\alpha_n^2 D_x - \alpha_n^2 s_j^2 D_1 F W_j), \tag{93}$$

$$F M_{xyj} = -D_{xy} \alpha_n^2 s_j F W_j , \tag{94}$$

$$F M_{yxj} = D_{yx} \alpha_n^2 s_j F W_j , \tag{95}$$

$$F V_{xj} = D_x \alpha_n^3 - (D_1 + D_{yx}) \alpha_n^3 s_j^2 F W_j , \tag{96}$$

$$F R_{xj} = D_x \alpha_n^3 - (D_1 + D_{xy} + D_{yx}) \alpha_n^3 s_j^2 F W_j , \tag{97}$$

$$F V_{yj} = (D_y s_j^3 - D_{xy} s_j) \alpha_n^3 F W_j - D_2 \alpha_n^3 s_j . \tag{98}$$

Elastic Rigidities of the Deck

Considering a multicell box-beam bridge deck without intermediate diaphragms (see Fig. 6), the flexural rigidities, D_x and D_y in the longitudinal and transverse directions respectively, may be defined in terms of moment per unit curvature and are independent of the value of the shearing rigidity S_B. For the calculation of D_x, the second moment of area of the longitudinal section is taken in the usual way. This value is expressed per unit width and then multiplied by the value of Young's modulus to give the flexural rigidity D_x. The corresponding flexural rigidity in the transverse direction is obtained from the top and bottom flanges of the deck.

The torsional rigidity D_{xy} is obtained by considering the shear flow in the multicell structure. For decks where webs and flanges are relatively small as compared with the dimensions of the deck, Wittrick's equation [7] may be used. For decks with six or more cells, the torsional rigidity may be obtained by neglecting the net shear flow through the internal webs since these are generally small; the effective shear flow is taken along the flanges and outermost webs. Thus Bredt's single-cell formula [8] may be used. The torsional rigidity is expressed per unit width and D_{xy} is taken as one-half of this quantity. If the deck is closed at the ends by diaphragms, then a similar approach may be used to calculate D_{yx} in the longitudinal direction.

The coupling rigidities D_1 and D_2 are both taken as Poisson's ratio times the contribution to D_y from the flanges.

The shear stiffness S_B may be obtained by considering a transverse slice of the deck of unit width subjected to equal and opposite shearing forces V_{y1} and V_{y2} at the ends as shown in Fig. 5. This isolated slice may be considered as a frame with points of contraflexure in the flanges midway between the

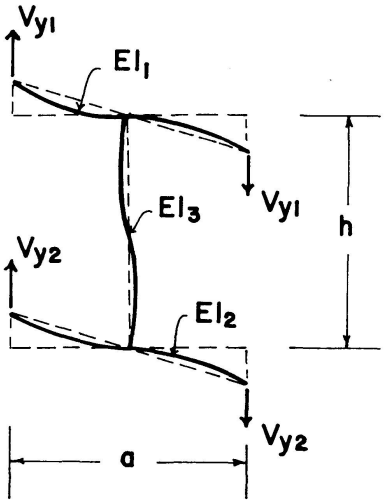

Fig. 5. Assumed frame deformation (Holmberg).

webs. HOLMBERG [9] has shown that for such a frame the shear stiffness S_B may be simplified to the form

$$S_B = \frac{1}{\frac{a\,h}{12\,E\,I_3} + \frac{a^2\,[3\,h\,(I_1+I_2)+a\,I_3]}{12\,E\,[12\,h\,I_1\,I_2+a\,I_3\,(I_1+I_2)]}}.$$

It will be appreciated that the assumptions involved in Holmberg's analysis are not completely realistic. However, in comparisons with more accurate analyses involving the use of computer programs for vierendeel frameworks, Holmberg's method has been found to give safe values for a range of web and flange dimensions. It is adopted here as a simple and conservative procedure for assessing shear stiffness.

Discussion of Results

In order to show the effect of vierendeel distortion on the load distribution characteristics of the deck, a twelve cell box-beam bridge deck is taken as an example. The dimensions are shown in Fig. 6 and the elastic rigidities in flexure, torsion and shear are calculated in the appendix.

The results are expressed in terms of distribution coefficients for deflection and moment. These coefficients were obtained by dividing individual values of deflection or longitudinal moment by their mean value as obtained from simple beam theory. For convenience the transverse bending moment is expressed in terms of the mean longitudinal moment. Using these elastic rigidities, the deck was analyzed with and without shear deformation and the

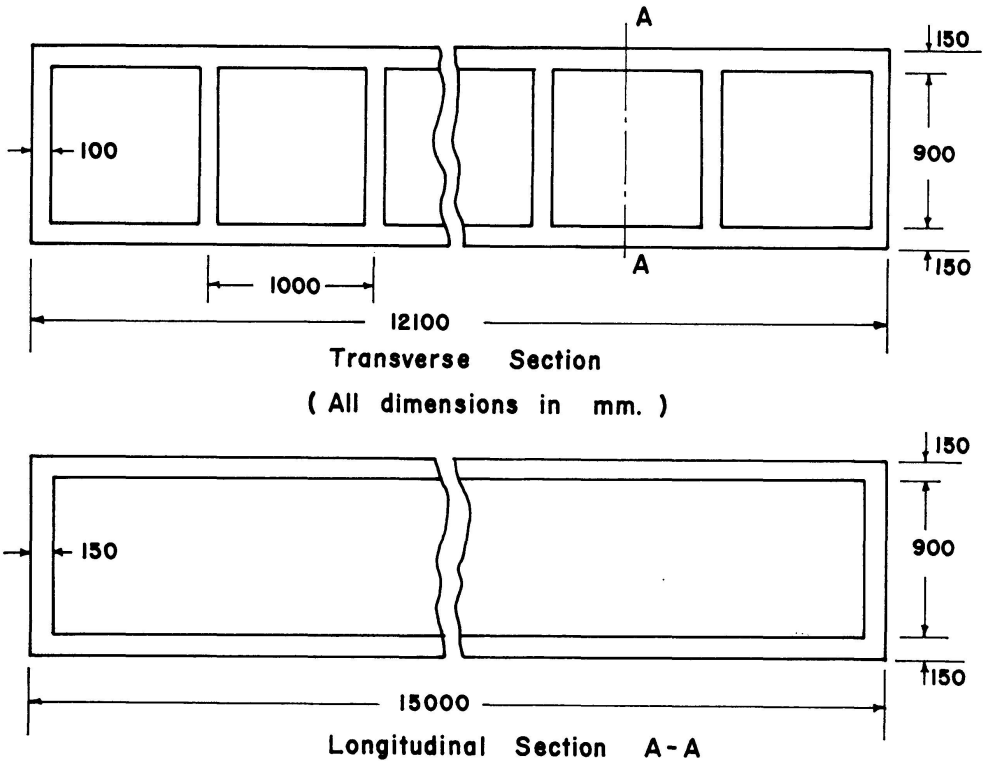

Fig. 6. Design example.

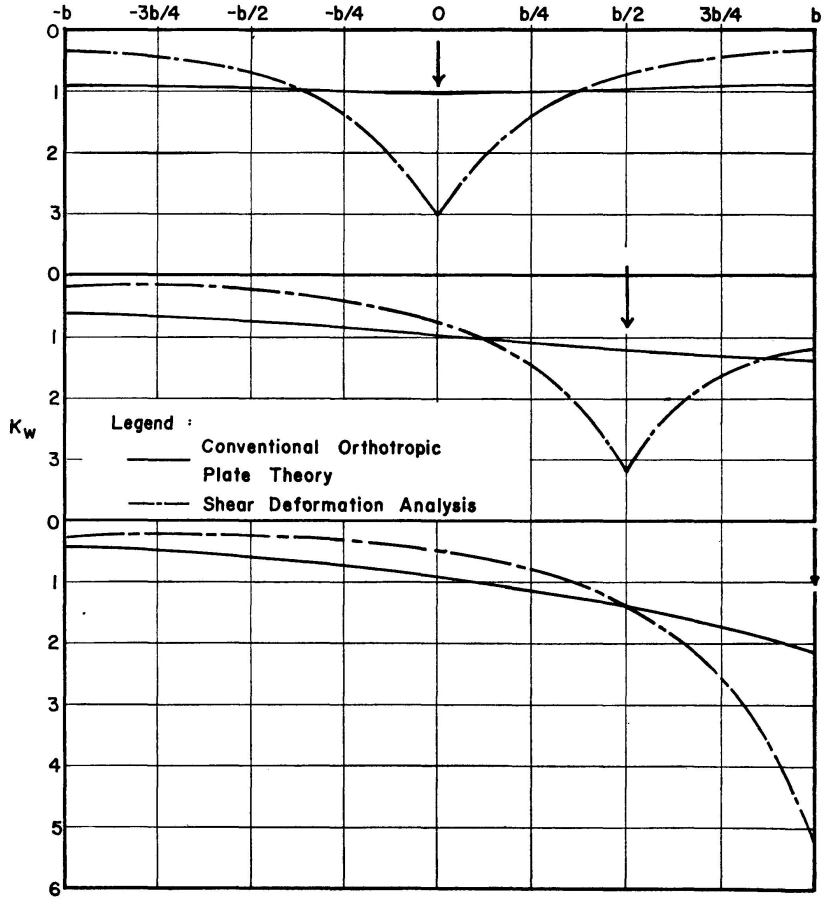

Fig. 7. Distribution coefficients for deflection.

results for central and two eccentric positions of concentrated load at midspan are shown in Figs. 7, 8 and 9. The values of deflection, longitudinal and transverse bending moment were computed using nine harmonics of the series. For the shear stiffness S_B, Holmberg's equation was used. From these figures

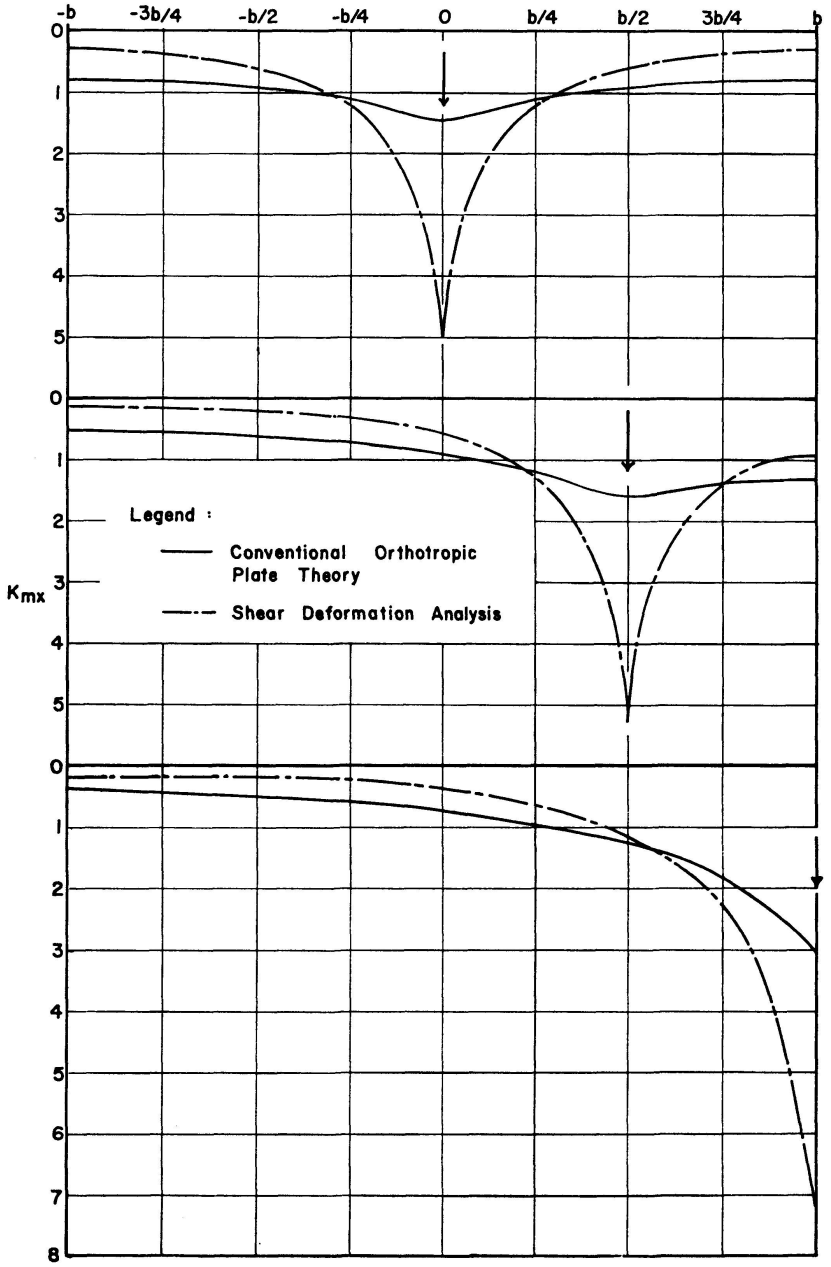

Fig. 8. Distribution coefficients for longitudinal moment.

it is apparent that the effect of vierendeel distortion on the deck is highly localized under the load. The peak values of the distribution coefficients for longitudinal moment vary from two to three times the corresponding values obtained using the conventional orthotropic plate theory, depending on the eccentricity of the load. A more realistic comparison may be made by con-

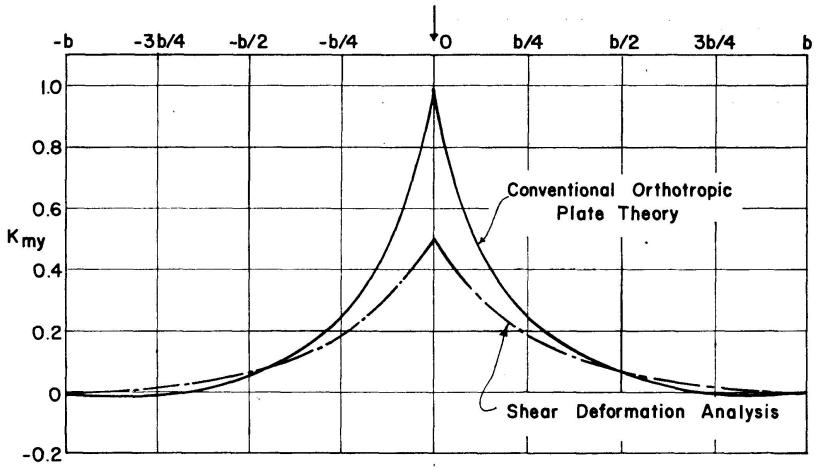

Fig. 9. Distribution coefficients for transverse moment.

sidering the areas under the curves. With the load at stations 0, $b/2$ and b, the percentage increases in the moment carried by the beams under these loads with the inclusion of the shear correction are 150, 126 and 86% respectively. This indicates the magnitude of the shear deformation effect and the necessity for taking account of it in design, especially when the webs of the multi-cell box beam bridge deck are fairly thin.

The presence of shear deformation decreases the peak value of transverse moment as shown in Fig. 9. This is to be expected as the shear stiffness S_B has the effect of reducing the overall rigidity of the deck in the transverse direction leading to a decrease of transverse moment.

The effect of shear stiffness on the load distribution characteristics of the

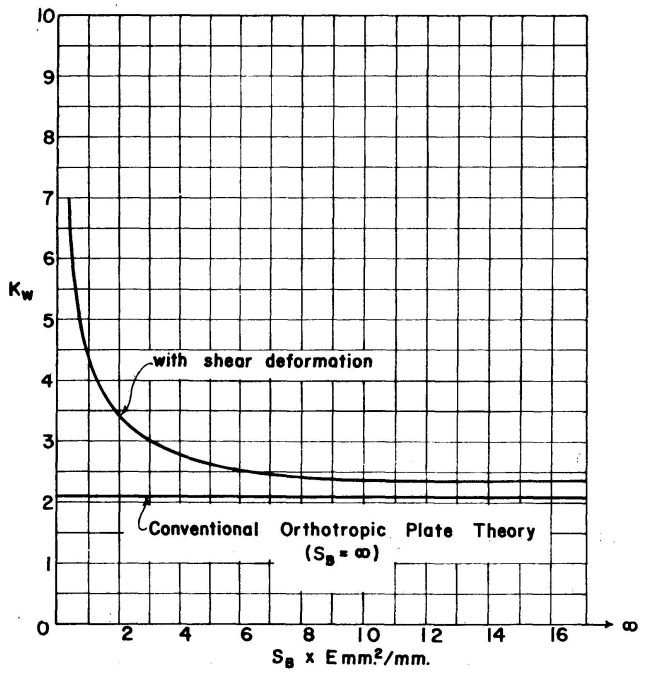

Fig. 10. Relation between peak value of distribution coefficient and shear stiffness.

deck is shown in Fig. 10. To illustrate this effect on the example bridge deck, values of S_B are plotted against the distribution coefficients for deflection. The load is placed at the edge to produce the peak value of distribution coefficient. For convenience the first harmonic only was considered. From this figure it appears that rapid increases in the value of $K_{w\,max}$ occur at low values of S_B. As the shear stiffness is increased the distribution coefficient approaches the value obtained from conventional orthotropic plate theory.

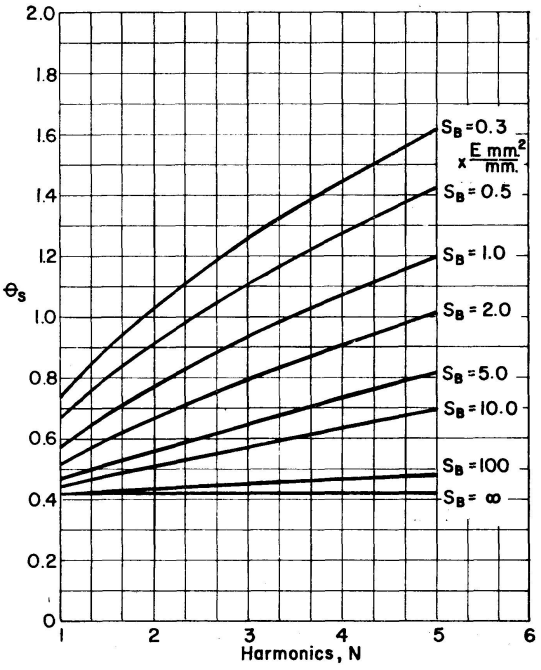

Fig. 11. Variation of flexural parameter θ_s with the harmonic.

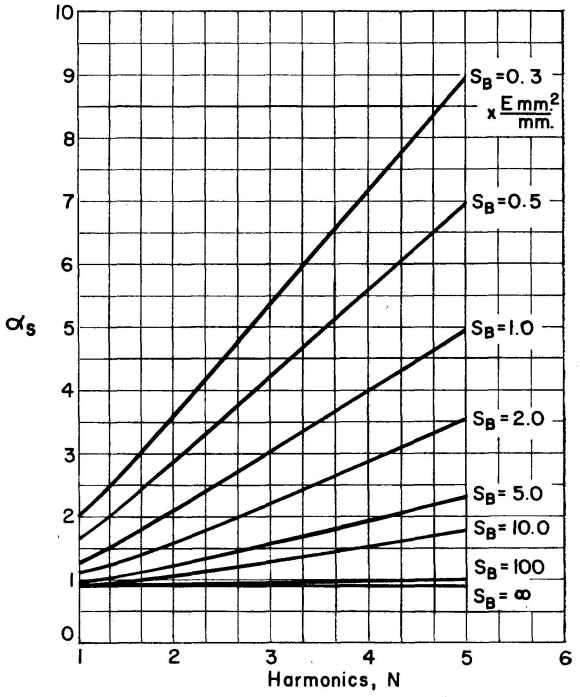

Fig. 12. Variation of torsional parameter α_s with the harmonic.

Figs. 11 and 12 are included to illustrate the effect of the number of harmonics on the values of the flexural and torsional parameters θ_s and α_s (Eqs. (39) and (41)). It is shown in the theoretical analysis that the parameters α_s and θ_s are functions of the harmonics. This makes it a difficult, if not impossible, task to reproduce the results in the form of design curves for the benefit of designers who do not have ready access to a digital computer. This can only be a practical proposition if distribution coefficients are obtained from the first harmonic of the series only. Experience has shown that up to nine harmonics are required in order to obtain accurate results with an analysis including shear deformation, especially for the values of moments and shears.

Conclusions

A theoretical analysis has been presented for determining the effect of vierendeel distortion on the load distribution characteristics of multicell box

beam bridges. It has been shown that this effect is somewhat localized in the vicinity of the load. Large increases in the peak values of longitudinal moment occur under the load as a direct consequence of vierendeel distortion, with an accompanying decrease in the transverse bending moment of the deck. Approximately, the increases in the peak values of deflection and longitudinal moment are inversely proportional to the shear stiffness of the deck. When S_B is infinitely large the values correspond with results from conventional orthotropic plate theory.

The flexural and torsional parameters have each been shown to be a function of the harmonics. The use of a digital computer is imperative for an accurate solution.

Acknowledgement

This work was carried out as an integral part of a research project on multibeam concrete bridge decks sponsored by the Construction Industry Research and Information Association. The authors are grateful to the Association for permission to publish these results in this form.

Appendix: Illustrative Example

The dimensions of the bridge deck are shown in Fig. 6. For the purpose of calculating the elastic rigidities of the deck in flexure and torsion, the value of Poisson's Ratio is taken as 0.15. The elastic rigidities are determined as follows:

$$D_x = \frac{1}{12}\left(1200^3 - \frac{900}{1000}\times 900^3\right) E = 89.325\times 10^6\, E \text{ mm}^4/\text{mm},$$

$$D_y = \frac{1}{12}(1200^3 - 900^3)\, E = 83.25\times 10^6\, E \text{ mm}^4/\text{mm},$$

$$D_1 = D_2 = \nu D_y = 0.15\times 83.25\times 10^6\, E = 12.49\times 10^6\, E \text{ mm}^4/\text{mm},$$

$$D_{xy} = \frac{1}{2}\times\frac{G\,4A^2}{b\oint\frac{ds}{t}} = \frac{G\times 4\,(12\,000\times 1050)^2}{2\times 12\,100\left(\frac{12\,000}{150}\times 2+\frac{1050}{100}\times 2\right)} = 63.06\times 10^6\, E \text{ mm}^4/\text{mm},$$

$$D_{yx} = \frac{G\times 4\,(14\,850\times 1050)^2}{2\times 15\,000\left(\frac{14\,850}{150}\times 2+\frac{1050}{150}\times 2\right)} = 66.50\times 10^6\, E \text{ mm}^4/\text{mm},$$

$$2H = (D_{xy}+D_{yx}+D_1+D_2) = 154.54\times 10^6\, E \text{ mm}^4/\text{mm}.$$

Using Holmberg's formula, the shear stiffness is obtained as

$$S_B = 0.834\, E \text{ mm}^2/\text{mm}.$$

For the conventional orthotropic plate theory the parameters α and θ are as follows:

$$\alpha = \frac{H}{\sqrt{D_x D_y}} = \frac{154.54}{2\sqrt{89.325 \times 83.25}} = 0.896,$$

$$\theta = \frac{b}{L}\sqrt[4]{\frac{D_x}{D_y}} = \frac{12100}{2 \times 15000}\sqrt[4]{\frac{89.325}{83.25}} = 0.410.$$

References

1. Y. GUYON: Calcul des ponts larges à poutres multiples solidarisées par des entretoises. Annales des Ponts et Chaussées, Vol. 24, No. 5, Sept.-Oct. 1946, p. 553.
2. C. MASSONNET: Méthode de calcul des ponts à poutres multiples tenant compte de leur résistance à la torsion. Publications, International Association for Bridge and Structural Engineering, Vol. 10, 1950, p. 147.
3. A. R. CUSENS, and R. P. PAMA: Distribution of concentrated loads on orthotropic bridge decks. The Structural Engineer, Vol. 47, No. 9, September 1969, p. 377–385.
4. C. MASSONNET, and A. GANDOLFI: Des cas exceptionnels dans la théorie des ponts à poutres multiples. Publications, International Association for Bridge and Structural Engineering, Vol. 27, 1967, p. 73–94.
5. F. SAWKO, and R. J. COPE: Analysis of multi-cell bridges without transverse diaphragms – a finite element approach. The Structural Engineer, Vol. 47, No. 11, November 1969, p. 455–460.
6. W. H. HUBER: Die Theorie der kreuzweise bewehrten Eisenbetonplatte nebst Anwendungen auf mehrere bautechnisch wichtige Aufgaben über rechteckige Platten. Bauingenieur, Vol. 4, 1923, p. 354.
7. W. H. WITTRICK: Torsion of a multi-webbed rectangular tube. Aircraft Engineering, Vol. 25, No. 298, Dec. 1963, p. 372.
8. R. BREDT: Torsion of tubular members. Z. Ver. Deut. Ing., Vol. 40, 1896, p. 815.
9. A. HOLMBERG: Shear-weak beams on elastic foundations. Publications, International Association for Bridge and Structural Engineering, Vol. 10, 1950, p. 69–85.

Summary

A theoretical analysis is presented for the analysis of multicell rectangular box beam bridges, without intermediate diaphragms, which considers the effect of Vierendeel distortion of the deck. The solution is expressed in Fourier Half-Range Sine Series and as such it is limited to simply supported bridge decks. The edges may be free or elastically restrained by edge beams of known elastic rigidities in flexure and torsion. The equations for deflection, moments and shears are derived and an illustrative example is included to show the effect of Vierendeel distortion on the load distribution characteristics of the deck. Comparison is made with conventional orthotropic plate theory.

Résumé

On présente une analyse théorique applicable au calcul des ponts en caisson multicellulaire sans entretoises, avec l'influence de l'effet de Vierendeel sur la chaussée. La solution est donnée sous forme de séries de Fourier et elle est limitée au cas des plaques simplement supportées. Les bords peuvent être libres, ou partiellement encastrés par des entretoises extrêmes de rigidités flexionnelle et torsionnelle connues. On établit les équations pour les flèches, les moments et les efforts tranchants; à l'aide d'un exemple, on montre l'effet de Vierendeel sur la répartition des charges sur la chaussée. On compare les résultats avec la théorie conventionnelle des plaques orthotropes.

Zusammenfassung

Es wird eine theoretische Analyse für die Berechnung mehrzelliger Kastenträger-Brücken, ohne Querscheiben, unter Beachtung der Vierendeelwirkung der Fahrbahn durchgeführt. Die Lösung wird in Fourier-Reihen ausgedrückt und ist auf einfach gelagerte Fahrbahnplatten begrenzt. Die Ränder können frei oder durch Endträger von bekannter Steifigkeit hinsichtlich Biegung und Torsion eingespannt sein. Die Gleichungen für Durchbiegung, Momente und Schub werden abgeleitet, und an einem Beispiel wird die Vierendeelwirkung auf die Lastverteilungscharakteristiken der Fahrbahn gezeigt. Zudem wird ein Vergleich mit der konventionellen orthotropen Plattentheorie angestellt.